

## Angular Momentum Partitioning and Hexacontatetrapole Moments in Impulsively Excited Argon Ions

H. M. Al-Khateeb, B. G. Birdsey, and T. J. Gay

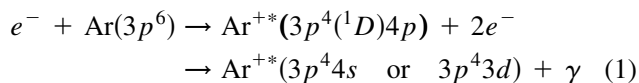
*Behlen Laboratory of Physics, University of Nebraska, Lincoln, Nebraska 68588-0111*

(Received 9 May 2000)

We have studied polarized electron collisions with Ar in which the target is simultaneously ionized and excited to form  $\text{Ar}^+(3p^4(^1D)4p)$  states. We measured the integrated Stokes parameters of the subsequent fluorescence emitted by the  $^2F_{7/2}$ ,  $^2F_{5/2}$ ,  $^2D_{5/2}$ , and  $^2P_{3/2}$  states along the direction of electron polarization. The Rubin-Bederson hypothesis is shown to hold for the  $L$  and  $S$  multipoles of these states. The electric quadrupole and hexadecapole of the  $^1D$  core are derived. By recoupling these moments with the electric quadrupole moment of the  $4p$  electron, we calculate higher moments of the total ionic orbital angular momentum, including its hexacontatetrapole (64-pole) moment.

PACS numbers: 34.80.Dp, 34.80.Nz, 34.80.Pa

Electron-atom scattering is a prototype of the many-body long-range force problem. Our understanding of collisions with H, He, and the light alkali atoms is good [1–3], but calculations of scattering from the heavy noble gases are not yet satisfactory [4–10]. This is due primarily to the outer  $p$ -shell configuration in such atoms and the fact that relativistic effects can be important in certain collision channels. While such targets present serious challenges to theory, they also provide a richer variety of physics to study. In this Letter, we examine a topic which has received little attention to date: the angular momentum partitioning between subshells of excited targets. We also report the first experiment of which we are aware that determines the hexacontatetrapole (64-pole) moment of an atomic system. Such studies hold the promise of providing information about scattering dynamics with unprecedented detail. To this end, we have studied the collision



using transversely polarized incident electrons, where the scattered electrons are not detected. This collision is particularly interesting because the residual target state is well  $LS$  coupled, unlike neutral Ar [11]. This simplifies the physical interpretation of our data, and reduces the difficulty for scattering theory in describing the target's final state, known to be a problem for neutral atoms [7,8]. Moreover, collision (1) involves simultaneous ionization and excitation of the target. Such collisions, long of interest for studies of ion lasers, have in the last few years come under renewed scrutiny because of the enhanced role played by electron correlation in this channel [4,12].

Our goal is to completely determine the distribution of angular momentum between the  $4p$  outer electron and the  $3p^4(^1D)$  core of the residual ion. To do this, we use irreducible tensor operators to describe the excited ion's electric and magnetic multipoles [13]. For our collision geometry, only a few multipoles are nonzero [14]. Furthermore, the "Rubin-Bederson" (RB) hypothesis (sometimes

mistakenly called the "Percival-Seaton" hypothesis [15]) states that if the process of ionizing and exciting the target takes place in a time significantly shorter than the time it takes the system to relax into its energy eigenstates, the collision can be considered as impulsively preparing the core, the outer electron, and the two continuum electrons independently. This reduces the number of subshell multipoles to four: the electric quadrupole and hexadecapole of the core, and the electric quadrupole and magnetic dipole of the  $4p$  electron. Assuming the RB hypothesis holds, the measurement of these moments constitutes a "perfect" experiment for this collision geometry.

In order to determine these multipoles, we measure fluorescence from the  $^2F_{7/2}$ ,  $^2F_{5/2}$ ,  $^2D_{5/2}$ , and  $^2P_{3/2}$  states. With the exception of the  $^2P_{3/2}$  level, whose core has a 12%  $^3P$  component [11], these are essentially pure Russell-Saunders states. They have energies of 36.90, 36.89, 37.26, and 37.11 eV above the ArI ground state, respectively. Knowing these energy levels, we can now assess the plausibility of the RB hypothesis. The duration of the near threshold ionization/excitation is of the order of the time it takes (ionized) electrons with an asymptotic energy of 2 eV to travel about three diameters of the residual ion, or  $\sim 6 \times 10^{-16}$  s. This time is a factor of 3 shorter than the "Coulombic relaxation time," i.e., the time it takes  $l_c$  and  $l_o$  to couple to form the total orbital angular momentum,  $L$ , as gauged by the biggest energy splitting in the manifold. The atom then relaxes into its fine structure in  $\sim 10^{-13}$  s, corresponding to the  $^2F_{7/2}$ - $^2F_{5/2}$  splitting. Thus the hypothesis is reasonable for this collision system, although perhaps marginally so for Coulomb relaxation.

The resultant multipole moments  $\langle \mathcal{T}_{KQ}^\dagger(L) \rangle$  of the coupled system's density matrix are given by [13]

$$\begin{aligned} \langle \mathcal{T}_{KQ}^\dagger(L) \rangle &= \sum_{\substack{kq \\ k'q'}} (kq, k'q' | KQ) \begin{Bmatrix} l_c & l_o & L \\ l_c & l_o & L \\ k & k' & K \end{Bmatrix} \\ &\times (2L+1) \sqrt{(2k+1)(2k'+1)} \\ &\times \langle \mathcal{T}_{kq}^\dagger(l_c) \rangle \langle \mathcal{T}_{k'q'}^\dagger(l_o) \rangle, \quad (2) \end{aligned}$$

where the  $(\dots|\dots)$  is a Clebsch-Gordan coefficient, and the  $\{\dots\}$  is a  $9j$  symbol. We can use Eq. (2) to write

$$t_{20}(L) = \frac{1}{1 + c_1 t_{20}(l_c) t_{20}(l_o)} \times \{c_2 t_{20}(l_o) + c_3 t_{20}(l_c) + c_4 t_{20}(l_c) t_{20}(l_o) + c_5 t_{40}(l_c) t_{20}(l_o)\}, \quad (3)$$

where  $t_{kq}(X) = \langle \mathcal{T}_{kq}^\dagger(X) \rangle / \langle \mathcal{T}_{00}^\dagger(X) \rangle$  is the “normalized” multipole moment, and the  $c_i$  are numerical coefficients which are different for each  $L$ . For  $L = 1, 2$ , and  $3$ , the coefficients are  $\{c_1, c_2, c_3, c_4, c_5\} = \{0.592, 0.100, 0.592, 0.120, 0.962\}$ ,  $\{-0.592, -0.592, 0.500, -0.505, -0.271\}$ , and  $\{0.169, 0.490, 0.828, 0.167, 0.037\}$ , respectively. These equations assume the validity of the RB hypothesis for the coupling of  $l_c$  and  $l_o$ , i.e., that the core and  $4p$  multipoles are uncorrelated. They thus form a complete set of nonlinear equations for the core hexadecapole  $t_{40}(l_c)$ , the core quadrupole  $t_{20}(l_c)$ , and the  $4p$  quadrupole  $t_{20}(l_o)$ . The equation for coupling the spin magnetic dipoles yields  $t_{11}(S) = t_{11}(s_o)$ .

In order to determine the individual electric multipole moments of the core and  $4p$  electron, we must make three independent photon measurements. This gives us sufficient information to use Eq. (3) to solve for  $t_{40}(l_c)$ ,  $t_{20}(l_c)$ , and  $t_{20}(l_o)$ . Since one-photon measurements yield information about multipole moments up to rank 2, analysis of a three-photon measurement including initial states with three different values of  $L$  provides information about tensors up to rank 6, or hexacontatetrapole moments, which are associated only with states having  $L \geq 3$ .

The  $L$  and  $S$  multipole moments couple into  $J$  moments, which are directly related to the Stokes parameters for linear and circular polarization through [14]

$$P_1 = \frac{3t_{20}(J)}{\{JJJ_f\}^{-1} \frac{(-1)^{J+J_f}}{\sqrt{2J+1}} \sqrt{\frac{8}{3}} + t_{20}(J)}, \quad (4)$$

and

$$P_3 = \frac{-3t_{11}(J) \{JJJ_f\}^{\{111\}}}{\frac{(-1)^{J+J_f}}{\sqrt{2J+1}} \sqrt{\frac{8}{3}} + \{JJJ_f\} t_{20}(J)}, \quad (5)$$

where  $J_f$  is that of the lower level of the transition in question and the  $\{\dots\}$  is a  $6j$  symbol.

There have been several other studies of collisionally produced hexadecapole moments in atoms [16,17], and three groups have used Stokes parameter measurements to study ionization/excitation collisions in the heavy noble gases [4,18–20]. To our knowledge, the present work represents the first study of angular momentum partitioning between shells of an excited state and the measurement of an atomic hexacontatetrapole.

Experimentally, we excite ground-state argon in a target cell and detect fluorescence along the electron polarization axis. The electron beam has an energy width of  $400 \pm$

TABLE I. Resonance transitions.

Transition	Wavelength (Å)	Filter wavelength (Å) (FWHM)
$4p^2 F_{7/2} \rightarrow ({}^1D)4s^2 D_{5/2}$	4609.6	4608(4)
$4p^2 F_{5/2} \rightarrow ({}^1D)4s^2 D_{5/2}$	4637.3	4637(5)
$4p^2 D_{5/2} \rightarrow ({}^3P)3d^2 D_{5/2}$	4481.8	4483(3)
$4p^2 P_{3/2} \rightarrow ({}^1D)4s^2 D_{3/2}$	4237.3	4237(4)

40 meV FWHM and a polarization of  $20.1\% \pm 0.3\%$ . We measure the fractional linear polarizations and circular polarization of the light (Stokes parameters  $P_1$ ,  $P_2$ , and  $P_3$ ) [13]. A description of our apparatus is given elsewhere [7]. Details of the transitions and interference filters we used to isolate them are given in Table I.

Figure 1 shows our results for  $P_3$  normalized to electron polarization, and  $P_1$ . We have restricted our measurements to energies within 3 eV of threshold for the states in question, to eliminate the effects of cascading from higher-lying levels. Using Eq. (2) with the replacements  $\{L, l_c, l_o\} \rightarrow \{J, L, S\}$ , Eqs. (4) and (5), and the data of Fig. 1, we can calculate values of the overall normalized electric quadrupole,  $t_{20}(L)$ , and magnetic dipole,  $t_{11}(S)$ , for the states in question. These results are shown in Fig. 2.

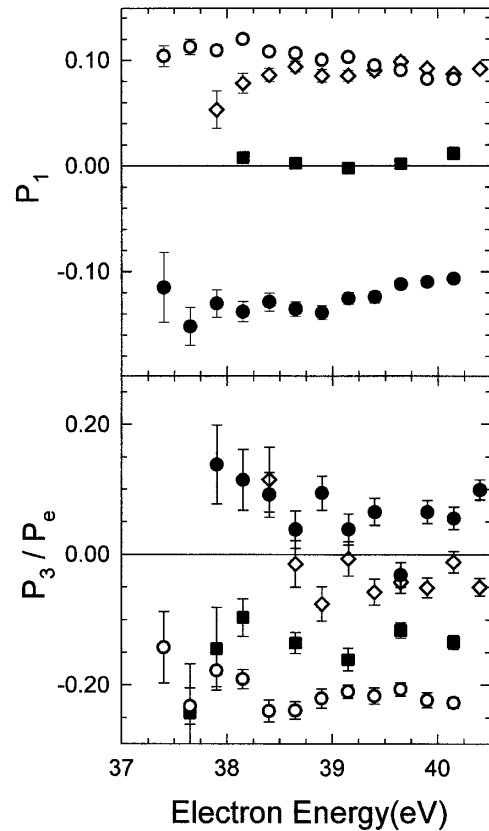


FIG. 1. Values of  $P_1$  and  $P_3$  (normalized to electron polarization), as a function of incident electron energy. Data legend for the excited states: open circles,  ${}^2F_{7/2}$ ; solid circles,  ${}^2F_{5/2}$ ; open diamonds,  ${}^2D_{5/2}$ ; solid squares,  ${}^2P_{3/2}$ .

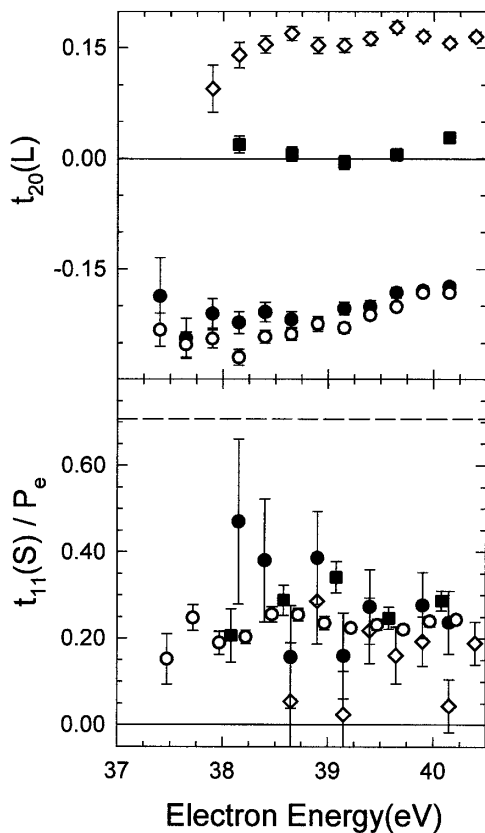


FIG. 2. Electric quadrupole [ $t_{20}(L)$ ] and spin magnetic dipole [ $t_{11}(S)$ ] moments of the Ar ion. The latter are normalized to electron polarization. Data symbols as in Fig. 1. For visual clarity, the open circles ( ${}^2F_{7/2}$  states) have been moved to the right by 67 meV, and the solid squares ( ${}^2D_{5/2}$  states) have been moved to the left by the same amount. The dashed line corresponds to the value of  $t_{11}(S)$  for pure exchange population of the  $4p$  level.

For  $LS$  target coupling, the RB hypothesis implies that the multipoles of  $L$  and  $S$  are independent, so states with the same  $L$  should have the same value of  $t_{KQ}(L)$ , regardless of  $S$  or  $J$ . Similarly  $t_{K'Q'}(S)$  should not depend on  $L$  or  $J$ . We see from Fig. 2 that the electric quadrupole moments for the  ${}^2F$  states,  $t_{20}(L = 3)$ , are nominally the same for both fine-structure components. A more stringent test of this idea is provided by the much broader energy scale

TABLE II. Electric multipole moments for the  ${}^1D$  core,  $4p$  “outer” electron, and composite  $L$  systems derived from the measured values of  $t_{20}(J)$  and  $t_{11}(J)$ .

Derived multipole moments	Incident Electron Energy		
	38.2 eV	39.2 eV	40.2 eV
$t_{20}(l_c)$	-0.09(2)	-0.061(8)	-0.028(5)
$t_{20}(l_o)$	-0.39(2)	-0.36(1)	-0.329(9)
$t_{40}(l_c)$	-0.28(4)	-0.19(3)	-0.24(2)
$t_{20}(L = 3)$	-0.25(2)	-0.219(8)	-0.179(6)
$t_{40}(L = 3)$	-0.09(2)	-0.06(1)	-0.09(1)
$t_{60}(L = 3)$	0.11(2)	0.07(1)	0.078(8)
$t_{20}(L = 2)$	0.14(2)	0.15(1)	0.156(6)
$t_{40}(L = 2)$	0.11(2)	0.08(2)	0.11(1)
$t_{20}(L = 1)$	0.018(12)	-0.0037(89)	0.0284(76)

of the  $3p^4({}^1D)4p$   $L$ -multiplet. By injecting spin into the ionic system using polarized electrons we find that  $t_{11}(S)$  is independent of  $L$  within the accuracy of our data. This demonstrates that the RB hypothesis holds for the  $L$  and  $S$  multipoles of the ion. Additionally, we found  $P_2$  to be consistent with zero for all transitions at all the energies we investigated, implying that  $LS$  coupling of the target holds and that spin-orbit coupling between the ion and the continuum electrons is negligible [7]. Figure 2 also shows the value of  $t_{11}(S) = 1/\sqrt{2}$  corresponding to collisions in which pure exchange excitation of the  $4p$  electron occurs. Since the measured value of  $t_{11}(S)$  is  $\sim 0.2$ , we conclude that core exchange and/or direct excitation of the  $4p$  state are the dominant collision channels.

The values of  $t_{20}(L = 1)$ ,  $t_{20}(L = 2)$ , and  $t_{20}(L = 3)$  allow us to use Eq. (3) to solve for the core and outer electron multipoles, which are presented numerically in Table II. The results do not vary significantly over the energy range we investigated, and it is clear that the shape of the core is dominated by its hexadecapole moment at all energies. This means that complete experimental investigations of collision dynamics of this type must generally assess such higher-order moments.

The nonlinearity of Eq. (3) means that multiple solutions for each set of the  $t_{20}(L)$  can exist. To address this issue, we used a terrain search Monte Carlo technique for the reported shell multipoles and their uncertainties [21].

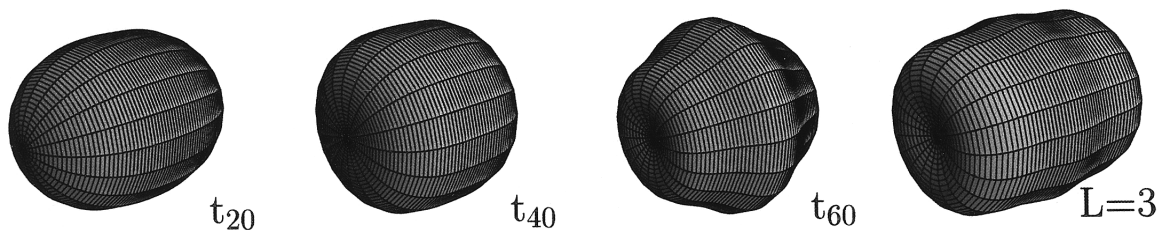


FIG. 3. Angular dependence of the  $L = 3$  ionic charge cloud before fine-structure relaxation. Incident electron energy = 40.2 eV. The radial coordinate of the cloud indicates the relative probability of finding an electron along a given direction. The pictures are normalized to the  $L = 3$  production cross section, and show the individual contributions of the electric quadrupole ( $t_{20}$ ), hexadecapole ( $t_{40}$ ), and hexacontatetrapole ( $t_{60}$ ) moments to the overall electron distribution.

The Monte Carlo technique determines the multidimensional distribution of probable solutions that results from the statistical uncertainty of the data. We found that the distribution of solutions at a given energy was well localized. The quoted multipole uncertainties reflect the size of this distribution. The assumption that there is no correlation between the individual core and  $4p$  multipoles cannot be checked experimentally in our case because there is no fourth redundant Eq. (3). The collision time is about one-third that of the Coulombic coupling time, so the RB hypothesis for the production of these multipoles is reasonable. Numerical results indicate that the range of possible solutions does not change significantly from the reported values when we include correlation in the analysis. However, residual effects due to correlation cannot be excluded categorically.

The orbital angular momenta of the collisionally excited core and  $4p$  electron couple quickly to form the various  $L$ -levels. The resultant  $L = 3$  state, for example, must be characterized by moments with ranks 2, 4, and 6. Using Eq. (2), we can derive these moments, which are also listed in Table II. In the case of the  $F$  state, the quadrupole, the hexadecapole, and the hexacontatetrapole all make significant contributions to the shape of the electron cloud. This is shown in Fig. 3.

We have demonstrated here a method for the determination of collisionally produced higher-order atomic multipole moments. The validity of the RB hypothesis for the  $L$  and  $S$  multipoles has been confirmed experimentally in the system studied here. In this regard, the injection of spin into the collision is important. The determination of the core and  $4p$  multipole moments elucidates the angular momentum partitioning in complex targets, and provides detailed data for the evaluation of state-of-the-art scattering theories.

We would like to thank D.H. Jaecks, O. Yenen, J.E. Furst, W.C. Moss, and W.C. Gay for useful discussions. This work was funded by the National Science Foundation under Grant No. PHY-9732258.

- 
- [1] T.N. Rescigno *et al.*, *Science* **286**, 2474 (1999).
  - [2] D.V. Fursa and I. Bray, *Phys. Rev. A* **52**, 1279 (1995).
  - [3] H.-L. Zhou *et al.*, *Phys. Rev. A* **52**, 1152 (1995).
  - [4] P.A. Hayes, D.H. Yu, and J.F. Williams, *J. Phys. B* **31**, L193 (1998).
  - [5] V. Zeman *et al.*, *Phys. Rev. A* **58**, 1275 (1998).
  - [6] J.E. Chilton and C.C. Lin, *Phys. Rev. A* **60**, 3712 (1999).
  - [7] B.G. Birdsey *et al.*, *Phys. Rev. A* **60**, 1046 (1999).
  - [8] X. Guo *et al.*, *J. Phys. B* **32**, L155 (1999).
  - [9] S. Kaur *et al.*, *J. Phys. B* **32**, 4331 (1999).
  - [10] C.M. Maloney *et al.*, *Phys. Rev. A* **61**, 22701 (2000).
  - [11] H. Statz *et al.*, *J. Appl. Phys.* **36**, 2278 (1965).
  - [12] R. Schwienhorst *et al.*, *J. Phys. B* **29**, 2305 (1996).
  - [13] K. Blum, *Density Matrix Theory and Applications* (Plenum, New York, 1996).
  - [14] K. Bartschat, K. Blum, and G.F. Kessler, *J. Phys. B* **14**, 3761 (1981).
  - [15] G. Csanak *et al.*, *Comments At. Mol. Phys.* **30**, 165 (1994).
  - [16] J.F. Williams, M. Kumar, and A.T. Stelbovics, *Phys. Rev. Lett.* **70**, 1240 (1993).
  - [17] A.G. Mikosza, in *Proceedings of the XXI International Conference*, edited by Y. Itikawa *et al.* (AIP, New York, 2000), Vol. CP500, p. 297.
  - [18] B.W. Moudry *et al.*, *Phys. Rev. A* **54**, 4119 (1996).
  - [19] K.W. McLaughlin, O. Yenen, and D.H. Jaecks, *Phys. Rev. Lett.* **81**, 289 (1998).
  - [20] P.N. Clout and D.W.O. Heddle, *J. Phys. B* **4**, 483 (1971).
  - [21] J.M. Chambers, *Computational Methods for Data Analysis* (Wiley, New York, 1977).